10th International Conference on Fracture Mechanics of Concrete and Concrete Structures
FraMCoS-X
G. Pijaudier-Cabot, P. Grassl and C. La Borderie (Eds)
https://doi.org/10.21012/FC10.235506

STRAIN DEVELOPMENT OF HIGH STRENGTH GROUTS UNDER COMPRESSIVE FATIGUE LOADING AND DETERMINATION OF FATIGUE PROPERTIES FROM SELF-HEATING MEASUREMENTS

ERISA MYRTJA*, OLIVIER RATEAU †, JEROME SOUDIER††, EVELYNE PRAT†† AND MOHEND CHAOUCHE†††

* LMT, ENS Cachan, CNRS, Université Paris-Saclay
Cachan, France
e-mail: erisa.myrtja@ens-cachan.fr, www.ens-paris-saclay.fr

† Civil Engineering Department, Université Paris-Saclay
Cachan, France
e-mail: olivier.rateau@ens-paris-saclay.fr, www.ens-paris-saclay.fr

†† Centre d'Innovation Parexgroup, Saint-Quentin-Fallavier, France
e-mail: evelyne.prat@parex-group.com, jerome.soudier@parex-group.com, www.parex-group.com

††† LMT, ENS Cachan, CNRS, Université Paris-Saclay
Cachan,France
e-mail: chaouche@lmt.ens-cachan.fr, www.ens-paris-saclay.fr

Key words: Fatigue, High-strength grout, Compression, Strain development, Heating

Abstract: Fatigue behaviour in concrete and grout has become a very important mechanical behaviour to be studied further due to more sleek structures requiring higher performances and strength, such as onshore and offshore wind turbines. However, relatively few studies are available about fatigue behaviour and often contradictory.

A series of monotonic and fatigue tests were performed to investigate the fatigue behaviour of ultra-high strength grout under compression. Multiple stress levels were tested at two loading frequencies, 10Hz and 1Hz. The developments of strain and stiffness degradation were analysed for each test and show a typical three-step damage mechanism.

At a higher frequency, some heating is observed within the specimen and the observations are made with thermocouples and infrared thermography. Since the fatigue testing is very time consuming, mostly when defining the S-N curve and endurance limit, an alternative method such as the self-heating method was used. This method is widely applied in materials such as steel [1], aluminium, composite materials or rubber-like materials, to define the endurance limit with only a few specimens based on the heating released during fatigue testing. To the authors knowledge, it has never been used in grout materials. Our experimental work on numerous specimens shows that the self-heating method might be an alternative method in order to predict the endurance limit for concrete and grouts.

1 INTRODUCTION

Modern constructions, influenced by developments in concrete technology, require higher performances of concrete, while being submitted to continuous cyclic loading during their service life. Thus the fatigue behaviour becomes a relevant and key factor to be analysed for structures such as bridges, railway slab tracks, offshore platforms and concrete pavements. Several studies have been focused on the fatigue behaviour of concrete and only recently on high performances concrete [2–4]. However, conflictual data are reported concerning the frequency effect, the number of cycles to failure with decreasing maximum stress level and their influence on strain development, generally due to the large scatter from fatigue testing and the heterogenous nature of concrete.

While fatigue in concrete is still subject of research, even fewer research is made on the behaviour of high strength grouts and mortars under fatigue lading. They are considered as fine-grained concrete with maximum grain size up to 6mm and can be used as connections in road joints or wind turbines. Cyclic loading due to continuous wind and wave loading make the joints prone to fatigue loading. Design methods developed for high strength concrete such as [5], which are based on Wöhler S-N curves, have not yet been proven to be applicable to high-strength grouts. Furthermore, reports from [6] consider different behaviours in fatigue loading between concrete and grout. Det Norske Veritas standard [7] serves as a guideline to describe the fatigue life in grouted connections for wind turbines. Nonetheless, additional testing is required to have a better understanding of fatigue damage mechanisms leading to fatigue failure.

An analysis of fatigue damage mechanism will be given by investigating the strain development during compressive fatigue under three maximum stress levels at two loading frequencies. Furthermore, the strains at failure in fatigue and quasi-static tests will be analysed.

Moreover, considerable temperature increase has been observed within grout specimens, depending on the frequency of testing applied and the maximum stress level. This may influence significantly the number of cycles to failure and is a parameter rarely observed from literature research. Fatigue tests being considerably long, authors usually apply high frequencies of testing, while neglecting the influence of specimen warming generated from fatigue testing at high frequencies.

The temperature increase in fatigue, can be used in order to determine the endurance limit which consists in applying the so-called "self-heating" method. While this method has been widely and successfully applied in materials such as steel, aluminium, composite materials or rubber-like materials [1,8–10], its application on grout might still be questionable mostly because the endurance limit concept has not been proven to exist in concrete or grout [11]. Model Code CEB-FIP [5] describes the fatigue behavior for $\log N > 10^8$ as asymptotically approach the minimum stress level, while DNV [7] is based on a change of slopes in the S-N curves. However, experimental tests conducted in this study show that this method might be used alternatively in order to estimate the endurance limit of a high-strength grout.

2 EXPERIMENTAL SET-UP

2.1 Mixture and specimen preparation

The experimental tests in this study were conducted on one mixture of high-strength grout, with an optimized particle packing structure. The optimization was performed by using the Andreasen modified model described as follows :

$$CPFT\,[\%] = \frac{D^q - D_s^q}{D_L^q - D_s^q} \qquad (1)$$

where CPFT is the "Cumulative Percent Finer Than". D_s / D_L describe the smallest / largest particle size and q is described as the distribution coefficient usually varying between 0,21 and 0,37, depending on the workability required. The mixture was established with a distribution coefficient of 0,3. This method has successfully been used in mortars and high strength concrete such as

[12,13]. The maximum grain size is set at 6mm and the water/binder ratio at 0,26.
Based on the grain size distribution obtained from Andreasen simplified model, where different grading curves were used and after the cement matrix optimization, the grout mix used for further testing is given as follows:

Table 1: Mixture Composition

Mix Composition	kg/m^3
Aggregate 0/6	2389
Limestone Filler	230
Cement	486
Silica Fume	77
Superplasticizer	6,7
Defoam	1,3
Water	72

The experimental tests were conducted on cylindrical specimens of 60mm in diameter and 120mm of height. The specimens were demolded 24 hours after casting and were stored in controlled conditions $T_{ambient}$ = 23°C for 8 weeks. The choice for testing at 8 weeks instead of 4, as usually is the case, was made in order to avoid variances of strength which can take place, since the fatigue tests can be relatively long. Thus, an experimental campaign lasting around 4weeks, has lower variances in strength between 8-12 weeks than those observed at 4-8weeks. Before testing a grinding machine is used on both circular faces, in order to ensure planar parallel faces and uniform stress distribution.

2.2 Equipment and measuring system

The compressive quasi-static and fatigue loading are conducted on a 500kN hydraulic MTS testing machine. The displacements are measured with laser distance sensors, where 3 of them are placed at a 120° angle to measure the longitudinal displacements and two are used to measure lateral displacements at mid-height of the specimen (see figure 1). The acquisitions were made at a frequency of 600Hz. Moreover, 4 type K thermocouples are used in order to measure temperature variations (2 on specimen surface and one at each compression platen). Additionally, in the self-heating tests, an infrared camera (JADE III IRFPA, resolution 320x256 pixels) was used in order to measure the temperature field.

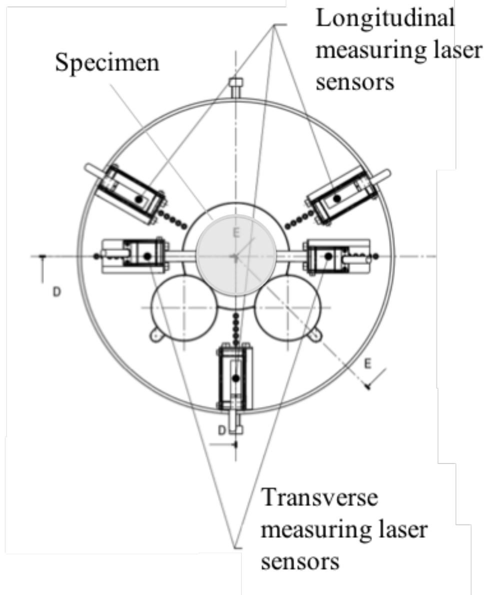

Figure 1: Plan view of the specimen equipped with displacement measuring laser distance sensors

2.3 Loading conditions

The compressive strength of the mixture is determined as the mean value of maximum stress obtained from 8 quasi-static tests. These tests are performed as displacement controlled tests with a loading rate of 3 µm/s. Considering that the number of cycles to failure from fatigue loading show significant scatter, 8 quasi-static tests are appropriate and sufficient. The maximum stress levels $S_{c,max}$ are expressed as a ratio of the maximum stress applied to the mean compressive strength and lie between 0,70 and 0,90. The stress ratio ($R = S_{c,min}/S_{c,\max}$) is kept constant for all tests at 0,1 and the waveform of loading between minimum and maximum stress level is sinusoidal. The fatigue tests were conducted under load control at two testing frequencies 10Hz and 1Hz . Finally, 6 specimens were tested until failure for each stress level.

3 RESULTS AND DISCUSSION

3.1 Fatigue life and influence of loading frequency

The number of cycles to failure are presented in figure 2 as a semi-logarithmic S-N curve and compared with the two standards mentioned earlier : DNV OS-J101 2014 [7] and CEB-FIP Model Code 2010 [5]. The linear regression of the number of cycles to failure at 10Hz is also plotted in figure 2, with its corresponding equation. 3 specimens were tested at $S_{c,\max}$ = 0,70 and did not fail up to 4x10^5 cycles. These specimens were not taken into account for the linear regression.

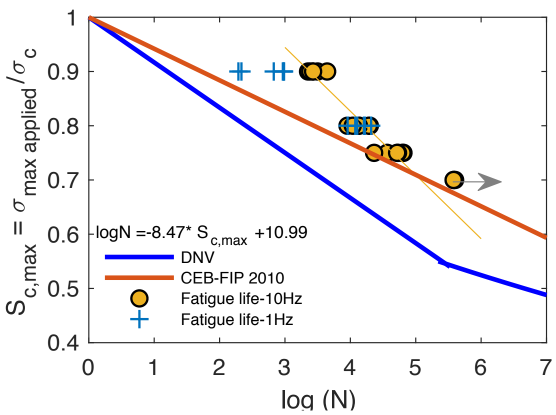

Figure 2: Fatigue life of high-strength grout and comparison with two standards

At two stress levels, fatigue tests were carried out at testing frequency 1Hz. A higher loading frequency leads to higher number of cycles to failure at $S_{c,\max}$ = 0,90. However, at $S_{c,\max}$ = 0,80 the number of cycles to failure are remarkably similar, but slightly higher at 1Hz when the mean values are compared. Whilst no tests were carried at lower stress levels at 1Hz, the tendency seems to change. Thus, higher number of cycles to failure are expected for lower stress levels. This results seems to be in accordance with [6,14], where the fatigue life increases at lower frequencies as the stress level decreases.

In fatigue tests, a higher frequency means that higher stress rates are applied and this can induce a viscous phenomenon at the cementitious matrix, which implicates a slight strength increase. This is also valid for quasi-static compressive tests [15]. The stress rate can be calculated as follows [16] :

$$\dot{\sigma_d} = 2f\,\Delta\sigma \qquad (2)$$

This equation shows that for higher loading frequencies and higher stress levels, the stress rates will reach higher values and thus a higher fatigue life. This is suggested in numerous articles in literature [17,18]. For high-strength grout and the loading conditions as described in this article, this suggestion seems valid for high stress levels. (>0,80). Nevertheless, at lower stress levels for loading frequencies at 10Hz, significant heating within the specimen is observed (detailed in part 3.3). The temperature gradients developed within the specimen and also the water within the specimen submitted under high pressure can lead to higher residual stresses, which may cause a decrease of the fatigue life.

3.2 Strain development under fatigue loading

In order to analyze fatigue deformation, the strain development of all tests was analyzed individually and a typical cyclic creep curve is shown in figure 3.

This curve shows the strain development during fatigue with respect to the normalized number of cycles to failure (N : current cycle ; N_f : number of cycles to failure), which is very similar to the strain development in creep under constant load.

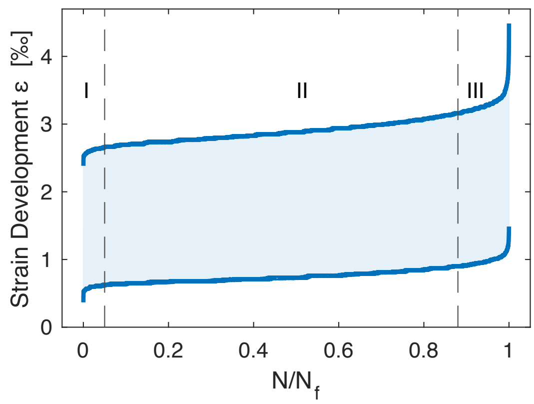

Figure 3: Typical cyclic creep curve

From literature research, authors unanimously agree that the strain development during fatigue is s-shaped and can be separated in three phases. This is also valid for high strength grouts as shown in figure 3, where the three phases are clearly distinguished. In phase I, the strain increases rapidly and it corresponds to the creation of microcracks. Subsequently, phase II is characterized by an almost linear increase of strain due to stable crack growth. Finally, in phase III the strain increases until failure due to the coalescence of microcracks.

An analysis of the transition phases between I-II and II-III showed that for higher stress levels, phases I and III are longer. The transition phases are defined more clearly by taking the derivative of each cyclic creep curve $\frac{\partial \varepsilon}{\partial n}$ as shown in figure 4.

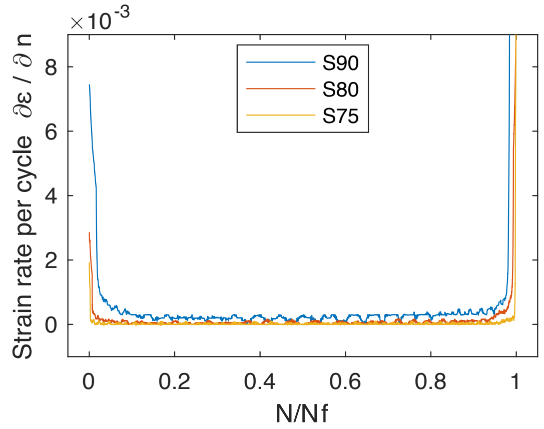

Figure 4: Typical relation between strain rate and ratio of number of cycles to number of cycles to failure for three stress levels

At $S_{c,max}$ = 0,90 transition I-II corresponds to 10% of the fatigue life, while it is 5% and 3% for $S_{c,max}$ = 0,80 and 0,75 respectively. The transition phase II-III occurs at 89%, 92% and 97% for $S_{c,max}$ = 0,90, 0,80 and 0,75 respectively. It could be explained by a more important internal damage caused at the beginning of the fatigue test, thus creating a longer phase I. During phase II the more numerous microcracks created in phase I propagate more rapidly until coalescence and failure of the specimen. This results differ from other literature data for concrete, where no uniform influence of maximum stress level on transition phases is found [18,19]. Nevertheless, only one author at [3] seems to agree that there is a prolongation of phase II with increasing number of cycles to failure.

The strains at failure in fatigue tests are compared with all quasi-static curves (shown as normalized stress) in figure 5. The ultimate strains in quasi-static tests $\varepsilon_{u,c}$ (strain at maximum stress) are shown as blue-hatched and are in the range of 3,66 ‰ and 4,15 ‰.

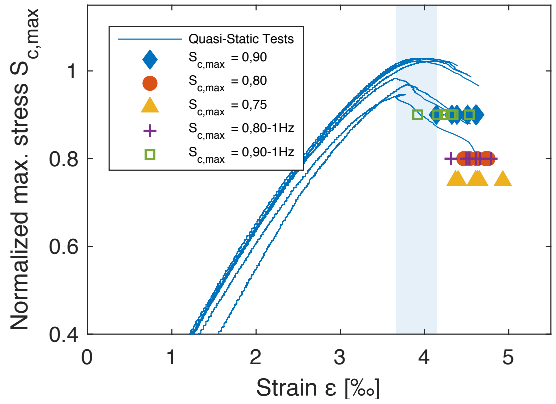

Figure 5: Quasi-static curves and strain at failure in fatigue

The strain at failure in fatigue increases while the maximum stress level decreases. For lower stress levels, the number of cycles to failure is higher and thus the time of testing is extended. Therefore, creep effects have a higher influence on the strain development. This is also assumed in [20,21].

Several fatigue life prediction models suggest that the fatigue failure is identified when the hysteresis loops reach the descending branch of the envelope curve [22]. However, conflictual results have been reported in literature, where the strain at failure in concrete can be lower [23,24] or higher [21] compared to the strain at failure from quasi-static tests. From figure 5 it was determined that around 85% of fatigue strains at failure are within the ranges of the strains at failure from quasi-static tests.

3.3 Temperature analysis

During fatigue testing it was observed that the repetitive loads result in specimen heating. Thus, all specimens were equipped with two thermocouples at mid-height (T_{th1} and T_{th2}) and two other thermocouples were placed at lower and upper platens (T_{lp} and T_{up}), in order to measure the temperature elevation by taking into account the heat transfer during loading. Therefore, the temperature increase of the specimen is given by :

$$\Delta\theta\ [K] = \frac{T_{th1} + T_{th2}}{2} - \frac{T_{up} + T_{lp}}{2} \tag{3}$$

The temperature increase at specimen's surface for all stress levels at f = 10Hz are given in figure 6. The specimens have a temperature increase up to $\Delta\theta$ = 30K in relation to the beginning of the test and up to 50°C as total temperature. Higher temperatures are reached for higher stress levels, which is due to a longer duration of test. However, the temperature increases much more rapidly during testing at higher stress levels. It is supposed that the heating comes from friction of internal microcracks. Thus, at higher stress levels, more cracks are generated at the beginning of the test and therefore more internal friction is created resulting in a higher temperature elevation.

Very few literature data are given on temperature increase due to compressive fatigue loading. However, similar results have been observed in [6] and [19] where the specimen's temperature increases up to 57K and 45K respectively. The higher values of temperature observed in these cases might be due to higher specimen dimensions (specimen height 180mm) and therefore the heat transfer between the specimen and the platens is slower.

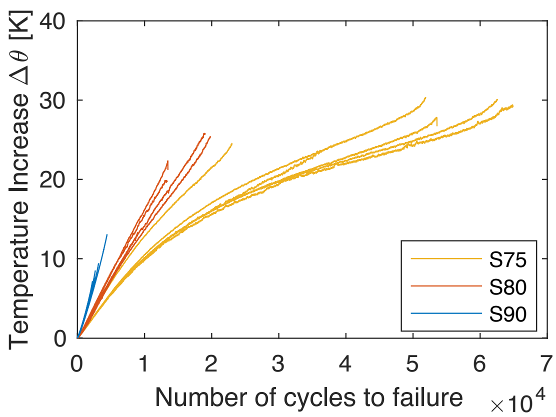

Figure 6: Temperature increase related to the number of cycles to failure

At a lower frequency f = 1Hz, the temperature increases more rapidly at the beginning of the test and stabilizes very quickly at a lower value than at 10Hz (cf figure 7). The temperature increase at higher frequencies might be a supplementary cause for fatigue life shortening.

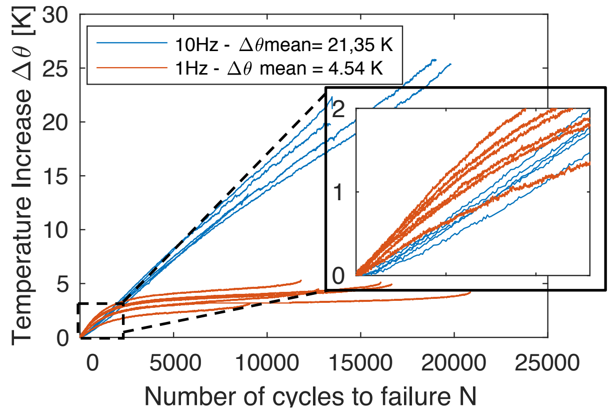

Figure 7: Temperature increase at two loading frequencies for $S_{c,max}$ = 0,80

4 SELF-HEATING METHOD

Fatigue tests as conducted earlier, are very consuming in time and specimen quantity. The duration of these tests can be extended further, if high-cycle fatigue tests are required in order to determine the endurance limit (level of stress under which the specimen does not fail under fatigue). Thus, alternative methods in order to characterize fatigue properties have been developed and the most widely used is the "self-heating" method. This method is based on measurements of the specimen temperature under fatigue loading in order to determine the endurance limit. The advantage of this method is the short time needed to perform the tests compared to the traditional high cycle fatigue tests [1].

The self-heating test consists in the application of a successive series of cyclic loadings, with increasing stress amplitude [8] and the stress ratio is kept the same. Every step is followed by an increase of temperature within the specimen until reaching a steady-state, where the temperature reaches a stabilized value $\bar{\theta}$ [K] (see figure 8). The last step is considered when the temperature does not reach a stabilized value. At first, the temperature increases rapidly as a result of a dissipated heating provoked by the loading, then stabilizes when a balance between dissipation and heat loss in the environment (air or platens) is established and finally it belatedly increases until failure during the propagation of the preponderant crack [25].

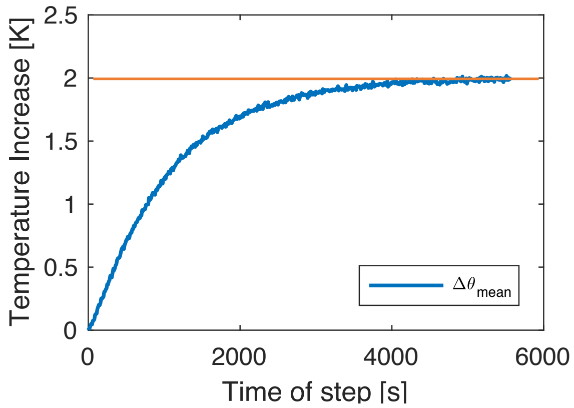

Figure 8: Estimation of the mean steady-state temperature during one loading step

The self-heating curve is obtained when the stabilized temperature is given with respect to the amplitude of stress applied . The endurance limit is estimated empirically from the intersection of two straight lines, one being the linear regression of the first three points and the second being the linear regression of the last 3 points. Thus, there are two clearly distinguished self-heating regimes, one of a small slope and a secondary slope associated with a progressive appearance of microplasticity areas [8]. It is supposed that the temperature increase comes from an intense microplastic activity, which at long term brings to the creation of multiple microcracks [25].

A few challenges were confronted in applying this method. In contrast to the steel materials, it is not generally accepted that an endurance limit exists in concrete or grout. Moreover, the specimen size in self-heating method for steel materials can be relatively small (e.g. [8] width = 10mm ; length = 120mm) because of a more homogenous nature and therefore reaching a steady-state temperature more rapidly. However for the grout mix studied here , no smaller dimensions can be taken, otherwise the specimen size would be considered as a non-Representative Elementary Volume (REV). Thus, the duration to reach the temperature stabilization will be influenced by the specimen size and also the thermal conductivity. Finally, it can be complicated to determine whether "the final" step has reached a steady state temperature. Since the estimation is made from the last 3 points of the self-heating curve, the value of the endurance limit can be inaccurate if the operator stopped the test earlier.

Prior tests not included here, showed that for the high strength grout tested here, steps of 55 000 cycles are necessary to reach a steady-state temperature. Figure 9 shows all 8 steps applied at a load ratio of R = 0,1 starting from $\sigma_{max,applied}$ at 25 MPa up to 95 MPa.

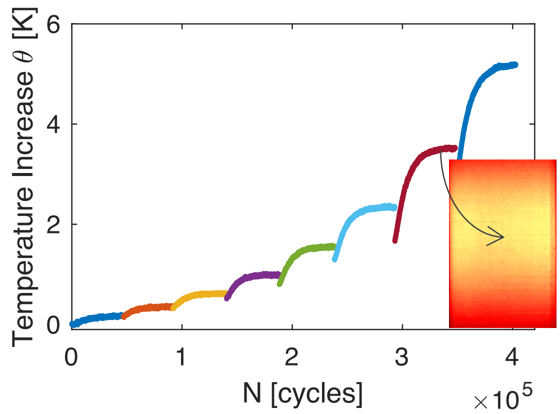

Figure 9: Variation of temperature increase for each step and example of temperature elevation at stabilized temperature with infrared camera

The endurance limit is identified empirically as the intersection between the linear regression of the last 3 points and the first 3 points. An example is shown in figure 10, where the endurance limit obtained for this specimen is of 67,3 MPa corresponding to $S_{c,max}$ = 0,40. The tests were conducted on five specimens and the values of endurance limits obtained show an error of 5%.

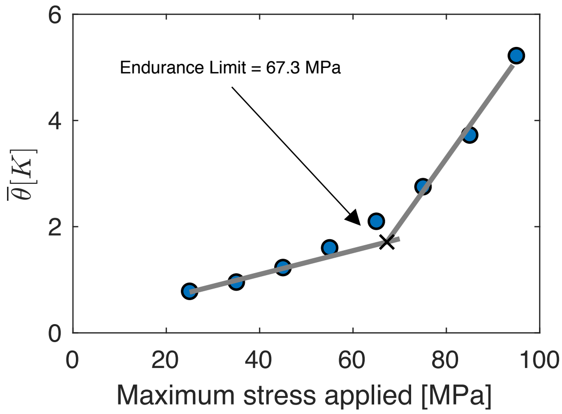

Figure 10: Typical self-heating curve and estimation of endurance limit

The figure 11 shows all fatigue tests at 10Hz and the mean endurance limit obtained from self-heating tests which is estimated at 0,39 as the mean value of five self-heating tests.

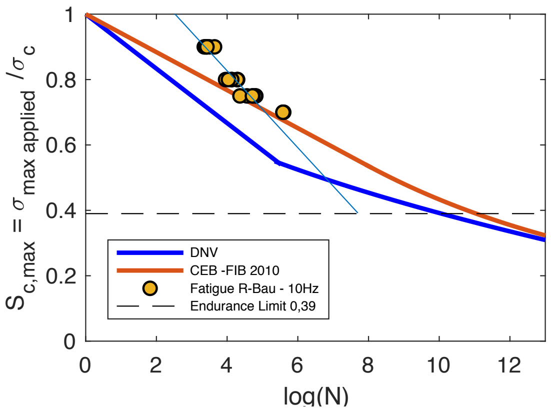

Figure 11: S-N curve, comparison with two fatigue standards and endurance limit estimated from self-heating tests

5 CONCLUSIONS

The present investigation is focused on the low-cycle compressive fatigue behavior of a high strength grout. Therefore, the number of cycles to failure, the temperature increase and the strain development were analyzed for different stress levels and two loading frequencies. As expected, it was found that for lower stress levels, higher number of cycles are obtained for both loading frequencies. However, different S-N curves are obtained at 1Hz, where for higher stress levels ($S_{c,max}$) lower number of cycles to failure are obtained. Nonetheless, the tendency changes for lower stress levels, where higher number of cycles to failure are expected for lower loading frequencies. This is partly due to the specimen heating observed in high frequency tests, which cause important temperature gradients and high pore water pressure within the specimen. This phenomenon rarely observed in concrete fatigue needs further investigation, in order to evaluate the level of influence on the number of cycles to failure and strain development.

Moreover, the analysis of the strain development shows that for higher stress levels, the phase I is expected to be longer due to more damaged caused, thus leading to a shorter time in cracks propagation time during phase II.

Additionally, the strain development and the strain at failure in fatigue is influenced by the maximum stress levels applied. It was found that higher number of cycles to failure, lead to higher maximum strains, which can be due to creep effects. Further fatigue tests at different loading frequencies and different specimen size need to be conducted in order to validate these hypothesis.

An alternative experimental method was applied, based on self-heating measurement in order to define the endurance limit in a grouted material. Firstly, the procedure was defined and it was noticed that larger fatigue loading steps are required in order to reach a steady state in temperature elevation compared to steel materials. However, the time needed to determine the endurance limit is minimized compared to traditional methods (a few hours instead of several days). The proposed experimental method showed very low scatter between the results obtained, however further validation is needed. Nonetheless, it seems as a promising method to be used in grout or concrete, in order to determine fatigue properties and the level under which failure might not occur.

REFERENCES

[1] C. Doudard, S. Calloch, P. Cugy, A. Galtier, F. Hild, A probabilistic two-scale model for high-cycle fatigue life predictions, *Fatigue Fract. Eng. Mater. Struct.* 28 (2005) 279–288.

[2] L. Lohaus, N. Oneschkow, M. Wefer, Design model for the fatigue behaviour of normal-strength, high-strength and ultra-high-strength concrete, *Struct. Concr.* 13 (2012) 182–192.

[3] N. Oneschkow, Fatigue behaviour of high-strength concrete with respect to strain and stiffness, *Int. J. Fatigue.* 87 (2016) 38–49.

[4] M.A. Vicente, D.C. González, J. Mínguez, M.A. Tarifa, G. Ruiz, R. Hindi, Influence of the pore morphology of high strength concrete on its fatigue life, *Int. J. Fatigue.* 112 (2018) 106–116.

[5] CEB-FIP, Model Code 2010 : Fatigue of concrete structures : State of the art report.

[6] K. Elsmeier, J. Hümme, N. Oneschkow, L. Lohaus, Prüftechnische Einflüsse auf das Ermüdungsverhalten hochfester feinkörniger Vergussbetone, B*eton- Und Stahlbetonbau*. 111 (2016) 233–240.

[7] DNV, Offshore Standard: Design of Offshore Wind Turbine Structures, 2014.

[8] R. Munier, C. Doudard, S. Calloch, B. Weber, Determination of high cycle fatigue properties of a wide range of steel sheet grades from self-heating measurements, *Int. J. Fatigue.* 63 (2014) 46–61.

[9] J.-C. Krapez, D. Pacou, Thermography detection of early thermal effects during fatigue tests of steel and aluminum samples, in: *AIP Conf. Proc*. 615, 2002: pp. 1545–1552.

[10] L. Jegou, Y. Marco, V. Le Saux, S. Calloch, Fast prediction of the Wöhler curve from heat build-up measurements on Short Fiber Reinforced Plastic, *Int. J. Fatigue*. 47 (2013) 259–267.

[11] M.K. Lee, B.I.G. Barr, An overview of the fatigue behaviour of plain and fibre reinforced concrete, *Cem. Concr. Compos.* 26 (2004) 299–305.

[12] S. V. Kumar, M. Santhanam, Particle packing theories and their application in concrete mixture proportioning: A review, *Indian Concr. J.* 77 (2003) 1324–1331.

[13] H.J.. Brouwers, H.. Radix, Self-compacting concrete: the role of the particle size distribution, in: *First Int. Symp. Des. Perform. Use Self-Consolidating Concr.* SCC 2005, Rilem, Changsha, Hunan, China, 2005: pp. 109–118.

[14] J. Hümme, C. von der Haar, L. Lohaus, S. Marx, Fatigue behaviour of a normal-strength concrete - number of cycles to failure and strain development, *Struct. Concr.* (2015).

[15] X. Zhang, G. Ruiz, R.C. Yu, E. Poveda, R. Porras, Rate effect on the mechanical properties of eight types of high-strength concrete and comparison with FIB MC2010, *Constr. Build. Mater.* 30 (2011) 301–308.

[16] L. Saucedo, R.C. Yu, A. Medeiros, X. Zhang, G. Ruiz, A probabilistic fatigue model based on the initial distribution to consider frequency effect in plain and fiber reinforced concrete, *Int. J. Fatigue.* 48 (2013) 308–318.

[17] B. Zhang, D. V. Phillips, K. Wu, Effects of loading frequency and stress reversal on fatigue life of plain concrete, *Mag. Concr. Res.* 48 (1996) 361–375.

[18] A. Medeiros, X. Zhang, G. Ruiz, R.C. Yu, M. de S.L. Velasco, Effect of the loading frequency on the compressive fatigue behavior of plain and fiber reinforced concrete, *Int. J. Fatigue.* 70 (2015) 342–350.

[19] C. von der Haar, S. Marx, Strain Development of plain High Strength Concrete under Fatigue Loading, in: *HiPerMat Ultra-High Perform. Concr. High Perform. Constrution Mater.*, 2016.

[20] C. von der Haar, S. Marx, A strain model for fatigue-loaded concrete, *Struct. Concr.* (2017) 1–9.

[21] A. Neville, Properties of concrete, 5th ed., Pearson, 2011.

[22] Y.J. Park, Fatigue of concrete under random loadings, *J. Struct. Eng.* (United States). 116 (1990) 3228–3235.

[23] M.A. Farooq, Y. Sato, T. Ayano, K. Niitani, Experimental and numerical

investigation of static and fatigue behavior of mortar with blast furnace slag sand as fine aggregates in air and water, *Constr. Build. Mater.* 143 (2017) 429–443.

[24] J.O. Holmen, Fatigue of concrete by constant and variable amplitude loading, University of Trondheim, 1979.

[25] M. Poncelet, Multiaxialité , hétérogénéités intrinsèques et structurales des essais d'auto-échauffement et de fatigue à grand nombre de cycles, Ecole Normale Supérieure de Cachan, 2007.